Deposition and Characterization of Transparent Thin Films of Zinc Oxide Doped with Bi and Sb

Antonino Gulino* and Ignazio Fragala*

Dipartimento di Scienze Chimiche, Università di Catania, V.le A. Doria 6, 95125 Catania, Italy

Received March 14, 2001. Revised Manuscript Received September 6, 2001

Undoped and Bi/Sb doped highly transparent ZnO films were grown adopting metal organic chemical vapor deposition with suitable combinations of $Zn(C_5F_6HO_2)_2{\cdot}2H_2O{\cdot}(CH_3OCH_2CH_2)_2O$, $Bi(C_6H_5)_3$, and $Sb(C_6H_5)_3$ precursors. Hexagonal ZnO phases were always found. Doping levels ranged from 1.4 to 7.4 and from 0.2 to1.8 atomic % for Bi and Sb, respectively. UV−vis measurements indicated that the film transmittance was usually as high as 90% in the visible and near-infrared region. Dopant surface segregation was found in X-ray photoelectron spectroscopy experiments. Preliminary resistivity measurements indicated that lightly doped ZnO films are semiconducting while greater doping levels could result in potential varistor properties.

Introduction

Zinc oxide (ZnO) thin films have a large number of useful opto- and acousto-electric properties[1] and are adopted in a variety of devices, including surface acoustic wave transducers,[2] optical waveguides,[3] varistors,[4,5] lasers,[6,7] gas sensors,[8,9] photoluminescent devices,[10−12] etc. More recently, they have been considered as an alternative to tin-doped indium oxide in solar cell windows due to the low cost and absence of any toxicity.[13−17]

ZnO represents an optical transparent conducting material[3,14−15,17] (TCO) due to the wide band-gap (∼3.3 eV) and propensity to defects or impurities.[12,18−21] Crystal defects, controlled by the syntheses procedures, strongly affect both optical[18] and electric properties.[21] Finally, *n*-type doping represents another convenient way to modify conduction properties.[8,15−17] Bi-doped ZnO represents, to date, the most important material for fabrication of varistors (ceramic variable resistors) whose technological applications are of growing relevance due to their highly nonlinear electrical characteristics. Since 1971, Matsuoka has described the essential features of semiconducting ZnO varistors on the basis of the addition of Bi_2O_3.[22] Alternative sets of dopant have been also adopted. Nevertheless, Bi_2O_3 has maintained a dominant role. Only one exception, based on Pr-doped ZnO, has been reported.[23] Moreover, small quantities of additional dopants increase the nonlinear electrical characteristics.[8,24−27] In particular, there is evidence that dopants affect the grain growth and introduce defect states that control the overall varistor characteristics.[24−32]

* To whom correspondence should be addressed. E-mails: agulino@dipchi.unict.it; lfragala@dipchi.unict.it.

(1) *Advanced Coatings & Surface Technology Alert*; John Wiley & Sons, Inc.: New York, 2000 (http://library-www.larc.nasa.gov/Larc/Alerts/coatings/coatings000303).
(2) Shih W.-C.; Wu, M.-S. *J. Cryst. Growth* **1994**, *137*, 319.
(3) Ohtomo, A.; Kawasaki, M.; Koida, T.; Masubuchi, K.; Koinuma, H.; Sakurai, Y.; Yoshida, Y.; Yasuda, T.; Segawa, Y. *Appl. Phys. Lett.* **1998**, *72*, 2466.
(4) Luo, J.; Wang, H.; Chiang, Y-M. *J. Am. Ceram. Soc.* **1999**, *82*, 916.
(5) Chiang, Y−M.; Wang, H.; Lee, J.-R. *J. Microscop.* **1998**, *191*, 275.
(6) Vispute, R. D.; Talyansky, V.; Choopun, S.; Sharma, R. P.; Venkatesan, T.; He, M.; Tang, X.; Halpern, J. B.; Spencer, M. G.; Li, Y. X.; Salamanca-Riba, L. G.; Iliadis, A. A.; Jones, K. A. *Appl. Phys. Lett.* **1998**, *73*, 348.
(7) Tang, Z. K.; Wong, G. K. L.; Yu, P.; Kawasaki, M.; Ohtomo, A.; Koinuma, H.; Segawa, Y. *Appl. Phys. Lett.* **1998**, *72*, 3270.
(8) Shimizu, Y.; Lin, F. C.; Takao, Y.; Egashira, M. *J. Am. Ceram. Soc.* **1998**, *81*, 1633.
(9) Weissenrieder, K. S.; Muller, *J. Thin Solid Films* **1997**, *300*, 30.
(10) Studenikin, S. A.; Golego, N.; Cocivera, M. *J. Appl. Phys.* **1998**, *84*, 2287.
(11) Dahan, P.; Fleurov, V.; Thurian, P.; Heitz, R.; Hoffmann, A.; Broser, I. *J. Phys.: Condens. Matter* **1998**, *10*, 2007.
(12) Egelhaaf, H.-J.; Oelkrug, D. *J. Cryst. Growth* **1996**, *161*, 190.
(13) Kazeoka, M.; Hiramatsu, H.; Seo, W.; Koumoto, K. *J Mater. Res.* **1998**, *13*, 523.
(14) Wu, X.; Coutts, T. J.; Mulligan, P. W. *J. Vac. Sci. Technol., A* **1997**, *15*, 1057.
(15) Palmer, G. B.; Poeppelmeier, K. R.; Mason, T. O. *Chem. Mater.* **1997**, *9*, 3121.
(16) Wang, R.; Sleight, A. W.; Cleary, D. *Chem. Mater.* **1996**, *8*, 433.
(17) Tang, W.; Cameron, D. C. *Thin Solid Films* **1994**, *238*, 83.
(18) Srikant, V.; Clark, D. R. *J. Mater. Res.* **1997**, *12*, 1425.
(19) Henrich, V. E.; Cox, P. A. *The Surface Science of Metal Oxides*; Cambridge University Press: Cambridge, 1994.
(20) Roth, A. P.; Webb, J. B.; Williams, D. F. *Phys. Rev. B* **1982**, *25*, 7836.
(21) Djembo-Taty, K.; Plaindoux, L.; Kossanyi, J.; Ronfard-Haret, J. C. *J. Chim. Phys.* **1998**, 95, 595.
(22) Matsuoka, M. *Jpn. J. Appl. Phys.* **1971**, *10*, 736.
(23) Mukae, K. *Am. Ceram. Soc. Bull.* **1987**, *66*, 1329.
(24) Clarke, D. R. *J. Am. Ceram. Soc.* **1999**, *82*, 485.
(25) Bernik, S.; Zupancic, P.; Kolar, D. *J. Eur. Ceram. Soc.* **1999**, *19*, 709.
(26) Ezhilvalavan S.; Kutty, T. R. N. *Mater. Chem.: Phys.* **1997**, *49*, 258.
(27) Agarwal, G.; Speyer, R. F. *J. Mater. Res.* **1997**, *12*, 2447.
(28) Luo, J.; Chiang, Y.-M. *J. Eur. Ceram. Soc.* **1999**, *19*, 697.
(29) McCoy, M. A.; Grimes, R. W.; Lee, W. E. *J. Mater. Res.* **1996**, *11*, 2009.
(30) Kim, J.; Kimura, T.; Yamaguchi, T. *J. Am. Ceram. Soc.* **1989**, *72*, 1390.
(31) Hng, H. H.; Knowles, K. M.. *J. Eur. Ceram. Soc.* **1999**, *19*, 721.
(32) Jacobsoone, V.; Follet-Houttemane, C.; Boivin, J. C. *Solid State Ionics* **1998**, *113−115*, 607.

10.1021/cm011088y CCC: $22.00
Published on Web 11/30/2001

Table 1. MOCVD Conditions

substrate temperature	320 °C
total pressure	2−6 Torr
O_2 gas flow rate	100 sccm
Ar gas flow rate	70−100 sccm
source sublimation temperature	120−125 °C
deposition time	30−60 min

Thin films of ZnO have been grown using a large variety of techniques, including metal organic chemical vapor deposition (MOCVD).[33] Recently, we have reported on MOCVD of ZnO films from the novel $Zn(C_5F_6HO_2)_2{\cdot}2H_2O{\cdot}(CH_3OCH_2CH_2)_2O$ liquid precursor and discussed the accurate reproducibility associated with constant evaporation (hence, constant mass-transport) rates for given source temperatures.[33]

In the present study, we report on MOCVD fabrication of Bi-doped ZnO, low Sb-doped ZnO, and, finally, Bi-doped ZnO with a low Sb content. In particular, our efforts have been focused on a simple route adopting a single multicomponent source in a monocomponent MOCVD reactor.

Experimental Details

The $Zn(C_5F_6HO_2)_2{\cdot}2H_2O{\cdot}(CH_3OCH_2CH_2)_2O$ adduct (hereafter $Zn(hfa)_2{\cdot}2H_2O{\cdot}$diglyme, hfa = 1,1,1,5,5,5-hexafluoro-2,4-pentanedionate ligand and diglyme = bis(2-methoxyethyl)-ether), was synthesized, purified, and characterized as already reported.[33] $Bi(C_6H_5)_3$ and $Sb(C_6H_5)_3$ (Alfa Products) (hereafter, $Bi\Phi_3$ and $Sb\Phi_3$ respectively) were used after sublimation in a vacuum.[34]

The thermal behavior of $Bi\Phi_3$ and $Sb\Phi_3$ was investigated by thermal gravimetric analysis (TGA) and differential TG (DTG), under prepurified nitrogen, using a 1 °C/min. heating rate, by means of a Mettler TA 4000 system equipped with a DSC-30 cell, a TG 50 thermobalance, and a TC 11 processor. A few milligrams of samples were accurately weighed and examined in the 30−450 °C range.

The MOCVD experiments were performed using an horizontal hot-wall reactor,[33] under reduced pressure. Appropriate mixtures of precursors were kept in recrystallized alumina boats. Optical transparent SiO_2 was used as substrate after cleaning in an ultrasonic bath with isopropyl alcohol. Pure Ar and O_2 were used as carrier and reaction gases respectively (Table 1). Moreover, additional H_2O vapors were used in order to facilitate the fluorine removal. The total pressure, maintained in the 3−5 Torr range, was measured using a MKS Baratron 122AAX system. Flow rates were controlled within ±2 sccm using MKS flow controllers and a MKS 147 Multi gas Controller.

Grain sizes were determined using XRD data and the Scherrer and Warren equation: $S = 0.9\lambda/(B\cos\vartheta_B)$,[35] where S is the grain size of the crystallite, λ is the wavelength of the X-ray source, and ϑ_B is the Bragg angle of the considered XRD peaks. B represents the fwhm line broadening obtained as follows: $B^2 = B^2_m - B^2_s$ where B^2_m is the fwhm line broadening of the material and B^2_s represents the fwhm line broadening of the standard (α-Al_2O_3).[35]

Doping levels were quantified by energy-dispersive X-ray (EDX) with a Link system.

X-ray diffraction (XRD) powder data were recorded on a Bruker D-5005 diffractometer operating in a $\theta-2\theta$ geometry (Cu Kα radiation 30 mA and 40 kV).

X-ray photoelectron spectroscopy (XPS) measurements were made with a PHI 5600 Multi Technique System (base pressure of the main chamber, 3×10^{-10} Torr). Resolution, correction for satellite contributions, and background removal have been described elsewhere.[36] XPS measurements required recovery of the 10^{-10} Torr base pressure in the analysis chamber due to some film outgassing during the sample loading.[36]

UV−vis spectra were recorded with a Perkin-Elmer Lambda 19 spectrophotometer.

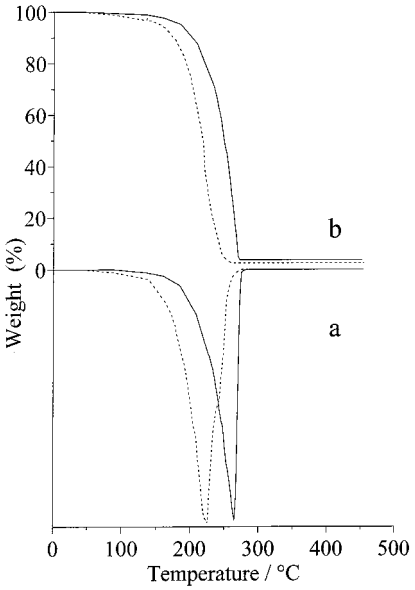

Figure 1. DTG (a) and TG (b) of both $Bi\Phi_3$ (dashed line) and $Sb\Phi_3$ (solid line) precursors.

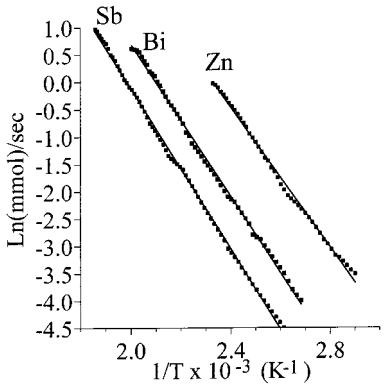

Figure 2. Arrhenius plot of the evaporation rates vs the reciprocal of evaporation temperatures of Zn, Bi, and Sb precursors.

Results and Discussion

We have already reported on the thermal behavior of the $Zn(hfa)_2{\cdot}2H_2O{\cdot}$diglyme adduct and results are consistent with its melting at 37.2 °C and evaporation of only one species, namely, the $Zn(hfa)_2{\cdot}$diglyme, with a peak temperature of 166.7 °C.[33]

TG and DTG analyses of $Bi\Phi_3$ and $Sb\Phi_3$ precursors both show (Figure 1) only one distinct peak at 226.0 and 264.3 °C, respectively. They account for sublimation processes. Some Bi_2O_3 residue (6%) has been found at 430 °C in the case of $Bi\Phi_3$. Almost no residue has been found in the case of $Sb\Phi_3$.

Figure 2 shows the Arrhenius plots of evaporation processes[37] of $Zn(hfa)_2{\cdot}$diglyme, $Bi\Phi_3$, and $Sb\Phi_3$. Linear

(33) Gulino, A.; Castelli, F.; Dapporto, P.; Rossi, P.; Fragalà, I. *Chem. Mater.* **2000**, *12*, 548.

(34) Gulino, A.; Compagnini, G.; Egdell, R. G.; Fragalà, I. *Thin Solid Films* **1999**, *352*, 73.

(35) Warren, B. E. *X-ray Diffraction*; Addison-Wesley: Reading, MA, 1969.

(36) Gulino, A.; La Delfa, S.; Fragalà, I.; Egdell, R. G. *Chem. Mater.* **1996**, *8*, 1287.

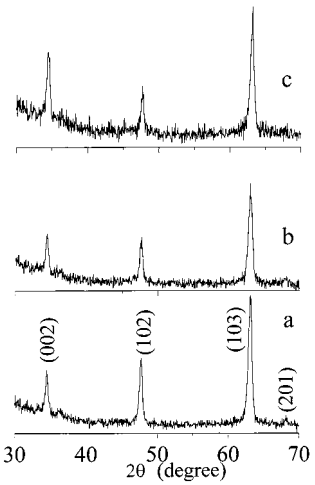

Figure 3. X-ray diffraction patterns, over a 30° < 2θ < 70° angular range, for SiO_2-supported, Bi−ZnO as-deposited thin films: (a) 1.6%, (b) 5.5%, and (c) 7.4% doping levels.

Table 2. EDX Quantitative Analyses

nominal doping level % in the mixture composition	1	3	5	10
	Metallic Atomic % from EDX			
Zn	98.4	96.9	94.5	92.6
Bi	1.6	3.1	5.5	7.4
Zn	99.8		99.4	99.2
Sb	0.2		0.6	0.8
Zn	98.2		95.7	94.1
Bi	1.4		3.7	4.1
Sb	0.4		0.6	1.8

correlations are always observed with 53.2, 54.5, and 59.5 kJ/mol activation energies, respectively, for the Zn, Bi, and Sb precursors. In this context, note that the lower volatility of both $Bi\Phi_3$ and $Sb\Phi_3$ render the precursors well suited for light MOCVD doping of ZnO films.

Bi-doped ZnO films were deposited using suitable mixtures of the $Zn(hfa)_2{\cdot}2H_2O{\cdot}$diglyme and $Bi\Phi_3$. Deposition parameters are listed in Table 1. The crude $Zn(hfa)_2{\cdot}2H_2O{\cdot}$diglyme adduct has been shown to self-generate the liquid Zn source that melts at 37.2 °C[33] and dissolves the quantities of $Bi\Phi_3$, as required in the present experiments. The control of doping levels (atomic Bi/Zn %) has been satisfactory achieved by varying the composition of the mixed source precursors as well as by optimizing the evaporation temperature. In present experiments, source precursors were evaporated at constant 120 °C during MOCVD of Bi−ZnO films, since in the narrow 120 ± 5 °C range the Bi doping level of deposited films depends on the composition of the source. EDX data (Table 2) agree well with this observation. In all experiments, the substrate temperature was maintained at 320 °C, and the deposition time was 30−60 min. The evaporation rate of source mixtures under these conditions was $1.1 \pm 0.1 \cdot 10^{-2}$ g/min.

Sb-doped ZnO films were deposited using similar mixtures of the Zn precursor and $Sb\Phi_3$ in identical MOCVD conditions. EDX compositional data of low Sb doped films are correlated to compositions of source precursors in Table 2.

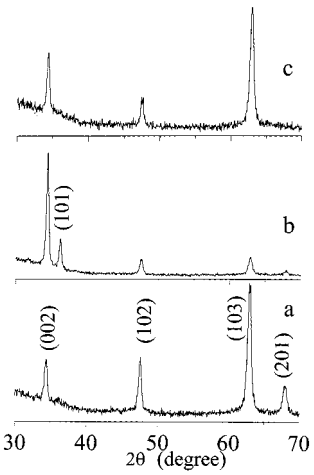

Figure 4. X-ray diffraction patterns, over a 30° < 2θ < 70° angular range, for SiO_2-supported, Sb−ZnO as-deposited thin films: (a) 0.2%, (b) 0.6%, and (c) 0.8% doping levels.

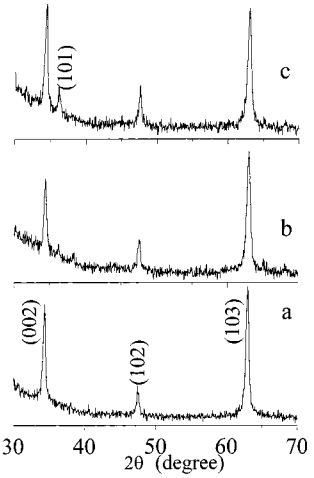

Figure 5. X-ray diffraction patterns, over a 30° < 2θ < 70° angular range, for SiO_2-supported, Bi/Sb−ZnO as-deposited thin films: (a) 1.4/0.4%, (b) 3.7/0.6%, and (c) 4.1/1.8% doping levels.

Mixed Bi/Sb doped ZnO films were fabricated by combining deposition parameters of single-dopant films. Thus, adopting 125 °C evaporation temperatures for multicomponent sources having nominal atomic compositions in the 0.5:0.5:99−5:5:90 Bi:Sb:Zn range, the Bi content in the films ranges from 1.4 to 4.1 atom %, while the Sb % is confined between 0.4 and 1.8 atom %. Relevant EDX data of films are compared to related source compositions in Table 2.

In all the present (as deposited) films, the fluorine and carbon contaminants, probed by EDX remain below 2%.

XRD measurements (Figures 3−5) of all as-deposited doped films provide evidence of hexagonal ZnO crystallites.[33,38] Moreover, the predominance of (002), (102), and (103) reflections points to some texturing.[33,38]

There is no XRD evidence of any Bi_2O_3 or Sb_2O_3 phases even at high doping levels. Note, in this context, that despite similarity of the ionic radii of Zn^{2+} and Sb^{3+}

(37) Garcia G.; Casado J.; Llibre J.; Figueras A. *J. Cryst. Growth* **1995**, *156*, 426.

(38) American Society for Testing and Material. *Powder Diffraction Files*; Joint Committee on Powder Diffraction Standards: Swarthmore, PA, pp 3−888.

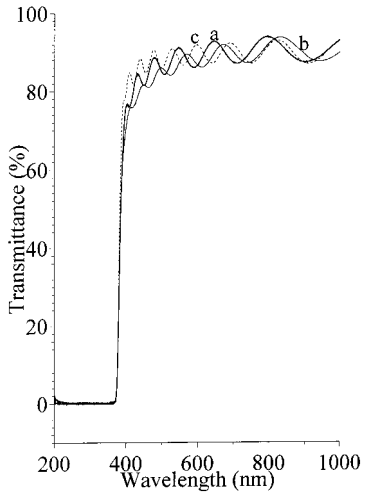

Figure 6. UV−vis transmission spectrum for 1.6% Bi-doped (heavy solid line a), 0.2% Sb-doped (light solid line b), and 1.4/0.4 Bi/Sb-doped (dashed line c) ZnO thin films on SiO_2 substrate.

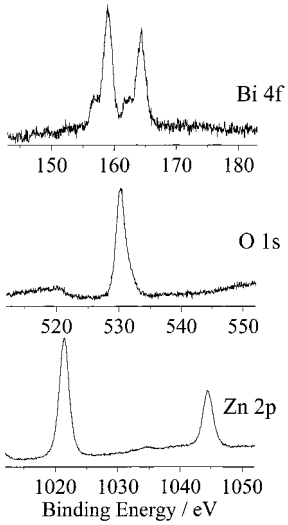

Figure 7. Al Kα-excited XPS of a 1.6% Bi-doped ZnO film measured in the (a) Zn 2p, (b) O 1s, and (c) Bi 4f energy regions. Structures due to satellite radiation havebeen subtracted from the spectra.

(0.74 and 0.76 Å),[39] the lattice parameters *a* and *c* (3.253 and 5.220 Å, respectively) measured in Sb-doped ZnO can be compared with $a = 3.249$ and $c = 5.206$ Å in pure ZnO.[38] In the case of Bi-doping (ionic radius of Bi^{3+} = 0.96 Å),[39] some cell expansion might be expected. In fact, values up to 3.258 and 5.220 Å were obtained for the lattice parameters *a* and *c* in Bi and Sb/Bi-doped ZnO. In particular, the hexagonal unit cell volume monotonically increases with the increasing of the doping level. In fact, values of 47.74, 47.75, and 47.79 $Å^3$ have been obtained for 0.2%, 0.6%, and 0.8% Sb-doped ZnO, respectively, while the 47.59 $Å^3$ value has been reported for pure ZnO.[38] For 1.6%, 5.5%, and 7.4% Bi-doped ZnO, values of 47.70, 47.76, and 47.87 $Å^3$, respectively, have been obtained. Sb/Bi-doped films show values almost identical, within the experimental uncertainty (±0.02), to those of Bi-doped analogues. In all cases, the increase in the unit cell volume indicates substitutional incorporation of the dopants into the ZnO host lattice. Moreover, the increased conductivity ($\rho = 4.64 \times 10^2$ Ω cm) of Bi-doped ZnO films (vide infra) is a further indication of substitutional alloying.

The crystallite sizes in doped ZnO films (determined from XRD)[35] deposited at 320 °C substrate temperature decrease from 21 to 17 (±2) nm upon increasing the Bi content both in Bi- and Bi/Sb-doped films. A similar behavior was previously observed for Bi/Sb-doped ZnO powders[27] as well as in Bi-doped ZrO_2 powders.[36] Sb-doped ZnO films have crystallite sizes of 28−29 (±2) nm and do not show relevant variation which depends on the different Sb-doping levels. In this context, the predominance of reflections (00*l*,*h*0*l*) perpendicular to the *c* axis in the diffraction patterns implies that the width of the dominant Bragg peaks mainly depends on the grain thickness in the c direction. In textured materials, the grain shape is usually anisotropic, therefore present values are to be considered only qualitative and not conclusive.

The deposited films are all transparent and their UV−vis spectra (Figure 6) find counterparts in earlier reported data.[3,14−15,17,40−43] In particular, transmittance always has a minimum at $\lambda \cong 370-377$ nm (the absorption edge) and increases to 90% in the visible and near-infrared range. The inferred band-gap lies within 3.30−3.35 eV. This observation appears to be of particular relevance for solar cell applications.[1]

The film thickness *d* was evaluated from UV−vis data using the classical equation[44] where n_1 and n_2 are the

$$d = \frac{\lambda_1\lambda_2}{2(\lambda_1 n_2 - \lambda_2 n_1)}$$

refractive indices at two adjacent maxima or minima at λ_1 and λ_2 wavelengths. Assuming $n_1 = n_2 = 2.0$ for hexagonal ZnO films,[33] the calculated *d* values are 950 and 1660−1700 nm for 30 and 60 min deposition experiments, respectively. The inferred growth rate of doped ZnO films is, therefore, 29 nm/min.

Figure 7 shows relevant XPS data of the 1.6% Bi-doped ZnO films. The Zn 2p features consist of the main $2p_{3/2}$, $2p_{1/2}$ spin−orbit components at 1021.4 and 1044.5 eV, respectively. The O 1s peak lies at 530.13 eV and shows a shoulder at 532.13 eV, possibly due to the presence of hydroxide species on the surface.[33,45−47] These features are identical to those already reported for related ZnO systems.[33,45−47] In the Bi 4f binding energy (B.E.) region, the B.E. values associated with the main peaks ($4f_{7/2} = 159.2$ eV and $4f_{5/2} = 164.5$ eV) and the spin−orbit splitting (5.3 eV) value are in good

(39) *CRC Handbook of Chemistry and Physics*, 65th ed; CRC: Boca Raton, FL, 1985.

(40) Vispute, R. D.; Talyansky, V.; Sharma, R. P.; Choopun, S.; Downes, M.; Venkatesan, T.; Li, Y. X.; Salamanca-Riba, L. G.; Iliadis, A. A.; Jones, K. A.; McGarrity, J. *Appl. Surf. Sci.* **1998**, *127−129*, 431.

(41) Oktik, S.; Russell, G. J.; Brinkman, A. W. *J. Cryst. Growth* **1996**, *159*, 195.

(42) Wark M.; Kessler, H.; Schulz-Ekloff, G. *Microporous Materials* **1997**, *8*, 241.

(43) Baird, T.; Campbell, K. C.; Holliman, P. J.; Hoyle, R. W.; Stirling, D.; Williams, B. P.; Morris, M. *J. Mater. Chem.* **1997**, *7*, 319.

(44) Swanepoel, R. *J. Phys. E: Sci. Instrum.* **1983**, *16*,1214.

(45) Mar, G. L.; Timbrell P. Y.; Lamnb, R. N. *Chem. Mater.* **1995**, *7*, 1890.

(46) Kim, S. J.; Marzouk, H. A.; Reucroft, P. J.; Hamrin, C. E., Jr. *Thin Solid Films* **1992**, *217*, 133.

(47) Schon, G. *J. Electron Spectrosc. Rel. Phenom.* **1973**, *2*, 75.

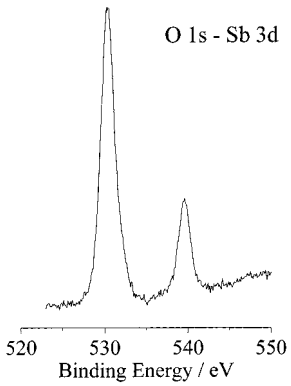

Figure 8. Al Kα-excited XPS of a 0.6% Sb-doped ZnO film measured in the Sb 3d−O 1s energy regions. Structures due to satellite radiation have been subtracted from the spectra.

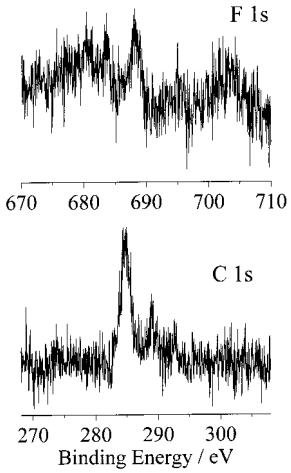

Figure 9. Al Kα-excited XPS of a 1.6% Bi-doped ZnO film measured in the C 1s and F 1s energy regions. Structures due to satellite radiation have been subtracted from the spectra.

agreement with data for both Bi_2O_3 powders[48] and vacuum-deposited Bi oxide films.[49] Two lower energy asymmetries are, however, apparent, and the associated B.E. values (157.2 and 162.3 eV) might be consistent with a surface phase already described as BiO.[36,49] As expected,[50−53] XPS spectra of the 0.6% Sb-doped ZnO films (Figure 8) have in the 525−545 eV region almost totally overlapped Sb $3d_{5/2}$ and O 1s peaks. The Sb $3d_{3/2}$ peak is, therefore, left for quantification of the surface Sb content.[50−54] No relevant differences were observed in the XPS spectra of ZnO films doped with both Bi and Sb cations.

XPS spectra of all samples show, in addition, sizable features due to fluorine and carbon surface contaminants (Figure 9) which are almost ubiquitous in similarly MOCVD fabricated materials.[45,54−55]

Zn $2p_{3/2}$, Bi 4f, Sb $3d_{3/2}$, O 1s, F 1s, and C 1s peaks, taken at 45° emission relative to the surface plane, were used to evaluate the effective surface atomic composition of as-deposited films, making due allowance for the relevant atomic sensitivity factors.[54] Remarkable Bi and Sb surface segregation were observed in all films with dopant surface atomic concentrations in the 15−30% range.[56] Greater segregation effects are observed for higher doping levels. This observation may be of some importance in view of varistor applications[24,28] since there is evidence that the varistor properties of ZnO do not depend on the amount of Bi^{3+} substitution. Rather, it is important that grain boundaries have adsorbed Bi_2O_3 layers.[57,58] Finally, quantification of the surface C and F contaminants results in 9 and 7 atom % contents, respectively, compared to the 2% probed by EDX in the bulk. Further film annealing at 400 °C in air brings down also the surface contaminants to less than 2%, leaving unaltered the XRD patterns.

Preliminary resistivity values, of air annealed films (with negligible contamination) were measured with a four probe system in the ±100 V range. There is evidence that undoped ZnO films are always insulating. The 1.6% Bi-doped ZnO films have 2.9 MΩ resistance. Making the due allowance for the 1.6 μm thickness, the resulting 4.6×10^2 Ω cm resistivity points to semiconducting films.[15,16,17,24,26,27,41] Similar results ($\sim 10^2$ Ω cm) were obtained for 1.4% Bi/0.4%Sb-doped ZnO films. In contrast, higher doping levels result in insulating ZnO films. A similar, counterintuitive observation has already been reported for ZnO powders having similar Bi and Sb doping levels and has been related to the smaller grain size associated to higher doping levels.[27] Moreover, it has been previously reported that 0.8% Al-doped ZnO thin films exhibit the lowest resistivity (7×10^{-4} Ω cm) while, resistivities up to 10^3 Ω cm have been observed upon increasing Al-doping levels (up to 4%).[17] Finally, opposite conductivity changes, which occur while increasing the doping level, have been previously reported also for other doped oxides.[19,50,51,59−61] In fact, ceramic pellets of 8% V-doped SnO_2 show a resistance of 3×10^7 Ω while, undoped SnO_2 pellets show a 7×10^5 Ω resistance value.[59]

Present highly doped films show greater dopant surface segregation which result in insulating Bi_2O_3/Sb_2O_3 surface layers and may also result in an increased resistivity.[62] This behavior is fundamental in view of varistor applications. In fact, highly insulating materials in the pre-switch region are required.[24]

(48) Morgan, W. E.; Stec, W. J.; Van Wazer, J. R. *Inorg. Chem*. **1973**, *12*, 953.
(49) Dharmadhikari, V. S.; SainKar, S. R.; Badrinarayan, S.; Goswami, A. *J Electron Spectrosc. Relat. Phenom*. **1982**, *25*, 181.
(50) Gulino, A.; Taverner, A. E.; Warren, S.; Harris, P.; Egdell, R. G. *Surf. Sci*. **1994**, *315*, 351.
(51) Gulino, A.; Condorelli, G. G.; Fragalà, I.; Egdell, R. G. *Appl. Surf. Sci*. **1995**, *90*, 289.
(52) A. Gulino, R. G. Egdell, I. Fragalà, *J. Mater. Chem*. **1996**, *6*, 1805.
(53) Gulino, A.; Egdell, R. G.; Baratta, G. A.; Compagnini, G.; Fragalà, I. *J. Mater. Chem*. **1996**, *6*, 1805.
(54) Wagner, C. D. Appendix 5. In *Practical Surface Analysis*, 2nd ed.; Briggs, D., Seah, M. P., Eds.; Wiley: Chichester, U.K., 1995.
(55) Gelius, U.; Heden, P. F.; Hedman, J.; Lindberg, B. J.; Manne, R.; Nordberg, R.; Nordling, C.; Siegbahn, K. *Phys. Scr*. **1970**, *2*, 70.
(56) Lee, J.-R.; Chiang, Y.-M.; Ceder, G. *Acta Mater*. **1997**, *45*, 1247.
(57) Morris, W. G.; Cahn, J. W. In *Grain Boundaries in Engineering Materials*; Walter, J. L., Westbrook, J. H., Woodford, D. A., Eds.; Claitors: Baton Rouge, LA, 1975.
(58) Kobayashi, K.-I.; Wada, O.; Kobayashi, M.; Takada, Y. *J. Am. Ceram. Soc*. **1998**, *81*, 2071.
(59) Egdell, R. G.; Gulino, A.; Rayden, C.; Peacock, G.; Cox, A. *J Mater. Chem*. **1995**, *5*, 499.
(60) Taverner, A. E.; Gulino, A.; Egdell, R. G.; Tate, T. J. *Appl. Surf. Sci*. **1995**, *90*, 383.
(61) Taverner, A. E.; Rayden, C.; Warren, S.; Gulino, A.; Cox, P. A.; Egdell, R. G. *Phys Rev. B* **1995**, *51*, 6833.
(62) Note that the thickness of the segregated layer is not enough to be revealed by XRD.

Conclusion

Highly transparent doped ZnO films have been successfully obtained by MOCVD using a liquid multicomponent source. Selection of suitable operating MOCVD condition proved capable of a fine control of the doping levels. All the as-deposited films consist of hexagonal crystallites with no Bi_2O_3 and Sb_2O_3 precipitates. Large transmittance properties (90%) have been found in the visible and near-infrared frequency region. Present films, therefore, are good candidates for large volume applications such as solar cells, flat-panel display, heat-reflecting coatings, etc. XPS measurements have shown dopant surface segregation, and this behavior appears of some importance in view of varistor applications. Preliminary resistivity measurements indicate that low doped ZnO films are semiconducting while higher doping levels result in insulating ZnO films. This observation clearly suggests that lightly doped films should behave as TCO while highly doped films represent potential ZnO varistors. Finally, to our knowledge, the present study represents the first example of MOCVD fabrication of Bi/Sb-doped ZnO.

Acknowledgment. Profs. F. Castelli, F. La Via, and G. Malandrino are grateful acknowledged for thermal, resistivity and EDX measurements, respectively.

CM011088Y